

# Innovative Analysis and Documentation of Gear Test Results

Pavel Žák and Vojtěch Dinybyl

## Management Summary

In this paper, a method is presented for analyzing and documenting the pitting failure of spur and helical gears through digital photography and automatic computerized evaluation of the damaged tooth flank surface. The authors have developed an accurate, cost-effective testing procedure that provides an alternative to vibration analysis or oil debris methods commonly used in conjunction with similar test-rig programs.

## Introduction

Modern industrial gearboxes often use nonstandard gear profiles to achieve reduced vibration and noise and to extend gear life. In this study, gearboxes and gear tooth designs were developed using the finite element method to predict gearbox deformations, shaft deflections and gear tooth deflections. Tooth profiles were optimized by simulation of gear mesh rotation, taking into account the aforementioned deformations and deflections.

To verify the design, a universal

experimental test stand was developed. The test stand was designed for shortened gear life, and tests were run for more than 2 million cycles. Factors analyzed included vibrations, torque and temperature, and the optimized gears were compared against samples designed using the DIN 3990 standard, method B.

After failing to develop a precise, time-saving and inexpensive method for confirming gear damage evaluation using various vibration methods (Refs. 1–2), a new method was developed based on visual analysis of the tooth surface.

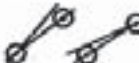
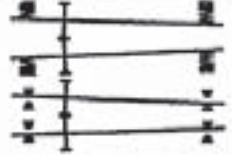
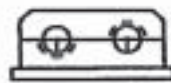
Phenomenon	Description	Phenomenon	Description
	a) Manufacturing deficiencies		d) Gear shaft deformations
	b) Gear shaft misalignment		e) Elastic deformations of gear body
	c) Bearing deformations and bearing imperfection		f) Deformations of housing

Figure 1—Main causes for the deviation of gear contact from the ideal line (Ref. 3).

## Gear Design Methodology

**Initial conditions.** Gearbox design and structure generally include shafts, gearwheels and bearings. All of these components have in their manufacture a defined, geometrical shape, which in turn influences the final three-dimensional position of the gearing.

Various geometric factors, including manufacturing deficiencies and tolerances of the bearings, shaft and housing can affect the positioning of gear teeth (Fig. 1). Every component has a specific stiffness, and its shape changes when a load is applied. The shaft (Fig. 1d) and gearbox (Fig. 1f) have considerable influence on the calculation procedure, as they can have the greatest effect on gear tooth contact. Although deformations in the bearings (Fig. 1c) and gear teeth (Fig. 1e) are less significant, they also must be considered.

In every mechanism where power is transmitted, mechanical loss changes to heat, which influences the structure and spatial configuration. Most affected by heat is the gearbox housing (Fig. 1f), but it is not the sole area warranting inspection; the whole system should be taken into account.

**Design procedure.** A modeling and calculating procedure (Fig. 2) derives from the possibility of partial task separation. Output parameters taken from previous steps can be used as next-step input parameters. Furthermore, those results can be incorporated into previous steps with the aim of design optimization. This method is presented in five separate steps in order to better accommodate user-friendly software.

**1. Calculation of gearbox housing deformations.** FEM mesh comes from CAD design, but actual manufactured dimensions are included. This mesh is virtually loaded by external forces created by reactions in bearing houses and force reactions from connection to ground frame. Also, deformations are influenced by the heat dilatation of the housing material. Calculation results are point positions, which characterize shaft positions.

**2. Calculation of shaft deformations.** The positions of shaft support points, calculated in Step 1, are used as input parameters. Another input is FEM mesh with respect to manufactured dimensions. The shaft mesh is virtually loaded by external forces supplied via gear meshing reactions. Calculation results are point positions, which characterize the position of shafts. The result is a spatial configuration of shafts.

**3. Calculation of gear deformations.** In this step, the gear and gear tooth deformations are calculated. The gear geometry and shaft positions are included in the calculation.

**4. Profile optimizing.** Simulation of gear mesh rotation is a part of this step. Mesh rotation is accomplished by rotation of the deformed gear on the deformed shaft. With the constant pressure method or spatial volume collision method, the modified tooth profiles

continued

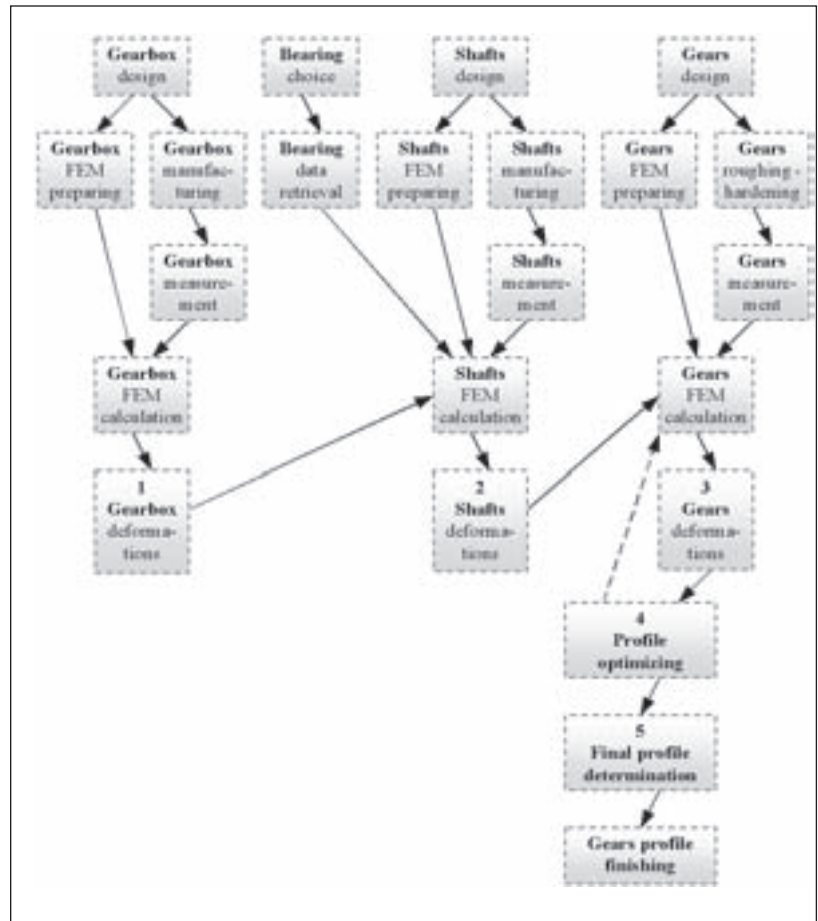


Figure 2—Methodology of gear design.

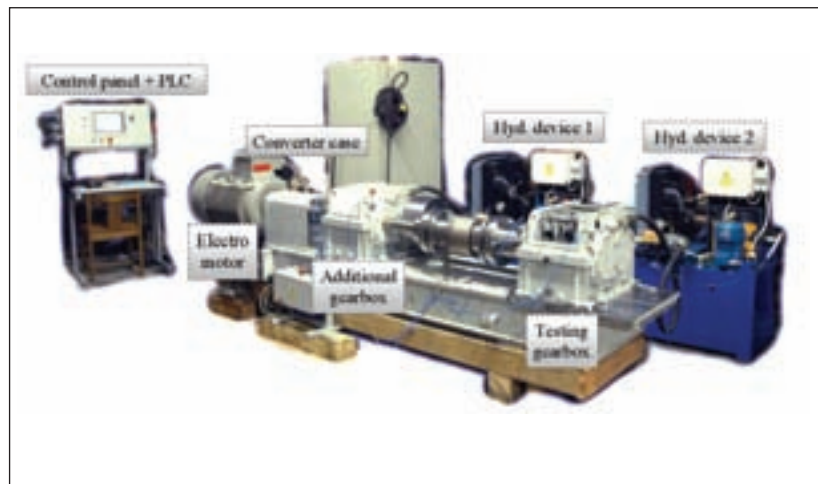


Figure 3—Photo of the complete experimental test rig.

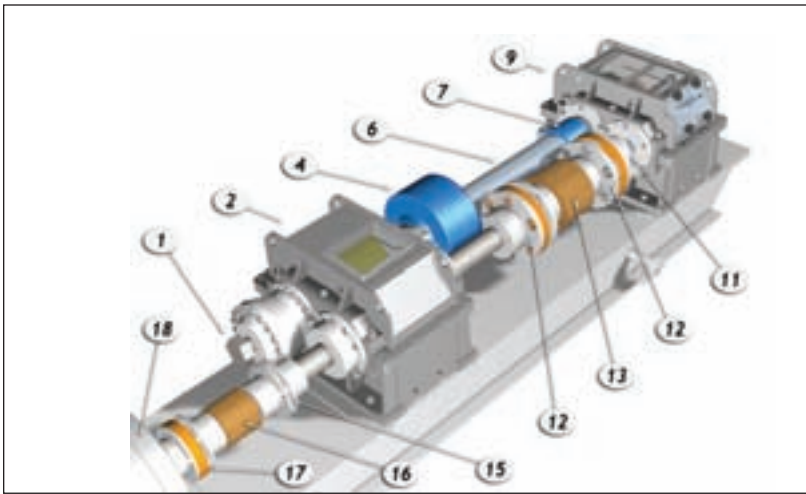


Figure 4—Visualization of test circuit (Ref. 5).

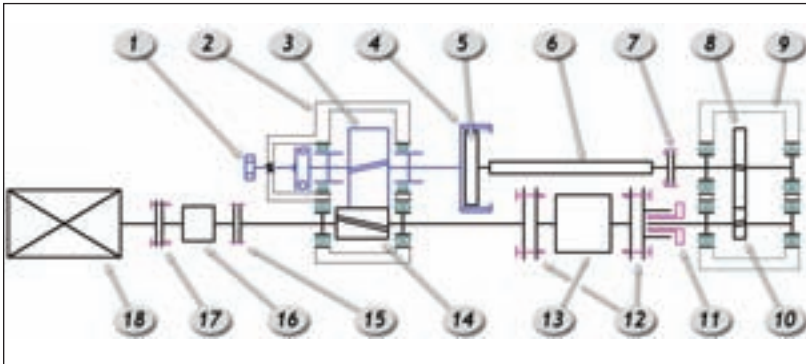


Figure 5—Schema of test circuit (Ref. 5).

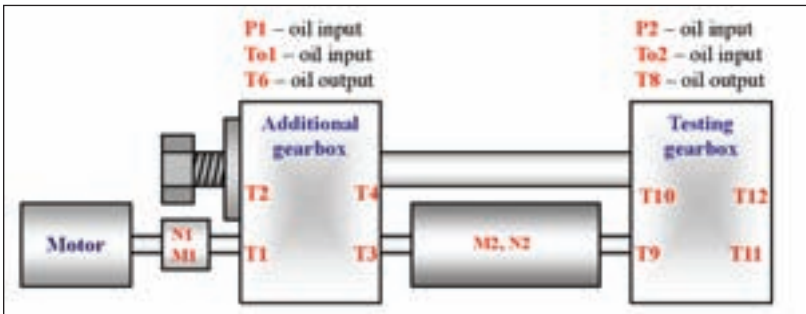


Figure 6—Placement of sensors.

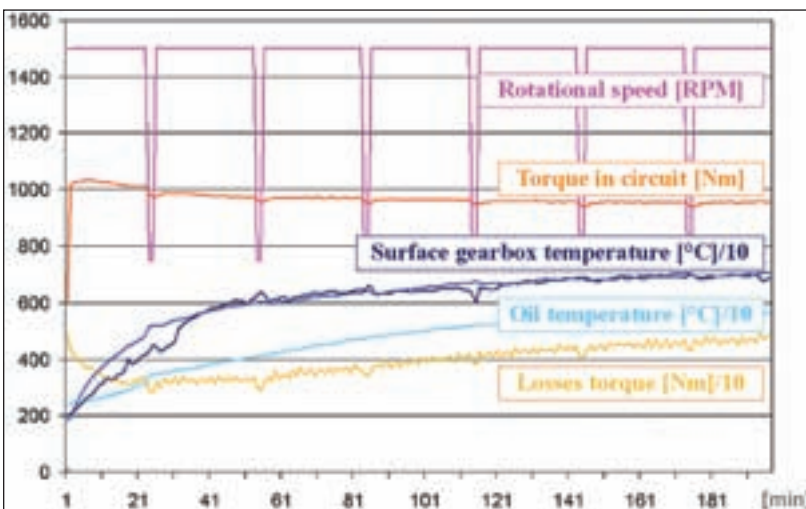


Figure 7—Illustrating test diagram.

are determined and ready for repeating of gear deformation calculations.

**5. Final profile determination.** Upon satisfactory results, the profile is converted to practicable technology for gear finishing, keeping in mind the corresponding tolerances.

#### Description of Experimental Stand

Niemann's back-to-back circuit is more energy-efficient than open loop. The testing circuit consists of measuring and additional gearboxes, driving motor, loading equipment, and sensors of torque, rotational speed, vibration and temperature. The torque in the circuit is established during stand operation. The test-rig is adjusted for possibility of geometry change for testing of pitting and tooth bending.

Testing conditions of gears and their assembly should be similar to actual operational conditions. To reduce testing duration, it is necessary to select a higher torque than would be used in industrial operation. In our case, we are limited by the torque sensor in the circuit, which allows torque up to 5,000 Nm. At 1,500 rpm, the circuit is dimensioned for maximum virtual power of 785 kW. Testing is mostly run on one load level for better results comparison. The complete test-rig with PLC, control panel, converter and hydraulic devices is shown in Figure 3. A schematic of the back-to-back circuit is shown in Figure 4, with a description of important elements in Figure 5.

**Circuit loading equipment.** Loading equipment must ensure readily available torque in the circuit, which is realized by axial movement of the gearwheel (Fig. 5, Pos. 3) with a helical gear in mesh with the pinion in the additional gearbox (Fig. 5, Pos. 14). This system is similar to that used at the NASA Glenn Research Center Spiral Bevel Gear Facility (Ref. 4). The tensioning screw gives rise to axial force that causes reaction (tangential force) in the gearing.

The tensioning screw moves the gearwheel that is fixed to the additional gearbox's low-speed shaft through an axial bearing. Axial freedom of movement occurs in the radial bearing with a long, nonstandard inner ring and in the gear coupling (Fig. 5, Pos. 4–5). The gear coupling is designed with a large diameter in order to decrease friction and contact stress among coupling teeth. At maximum torque, the axial force at the screw can be greater than 50,000 kN. This force is caused by friction between moveable contact surfaces.

It is possible to preset or slightly correct

the torque to the demanded value during the running period. The driving motor (Fig. 5, Pos. 18) is controlled by a frequency converter and only serves to provide for lost circuit power. The motor must be dimensioned for high running-up power.

**Torque sensors and other circuit parts.** Power losses and virtual power in the circuit during running are recorded by two rotational speed sensors and two torque sensors (Fig. 5, Pos. 13 and Pos. 16). As there is no live observation during the testing, an overload safety is needed. Torque sensors are mechanically secured against overload. Tooth root break can occur during testing of tooth bending fatigue, and the inertia moment can exceed the torque sensor's permissible overload during an unexpected gear failure. Maximum overload is 150% of nominal torque.

Breakable screws, which are parallel with the coupling axis, are used for security against torque sensor damage. The test gearbox is divided in two parts for easier test gear change. A coupling of involute splines (Fig. 5, Pos. 7) and ETP-Techno coupling (Fig. 5, Pos. 11) is used for securing the simple connection of the gearbox to the circuit.

**Automation of Control and Measurement Data Storage**

**Process loading of gearwheels.** The process load used for testing is determined by the expected gear loading during its expected lifetime. It consists of different limited time periods, according to these operating phases: run-up, steady regime, braking, run-out, idle regime, overloading, etc. The loading regime has to be determined in advance, with specific torque and rotation speeds for set periods of time. To control these actions, automation is needed.

For controlling rotation speed, we used a motor converter controlled by PLC. As mentioned, the torque in the circuit (Fig. 6 - M2) can be changed during operation by the axial screw. Although the authors used a wrench to adjust the axial screw, the design of the device allows for an automatic solution using an additional PLC-controlled motor and worm gearbox.

At the start of the test, it is possible to set up desired automatic periods through the use of a touch screen interface.

**Measurements of global values.** Measurement of torque (Fig. 6 - M1, M2), rotational  
continued

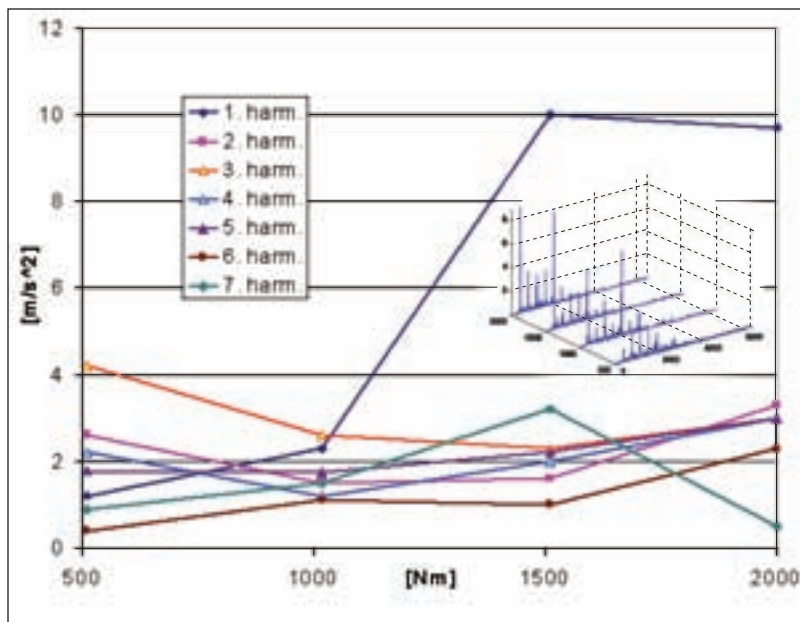


Figure 8—Relation between vibrations and moment in circuit.

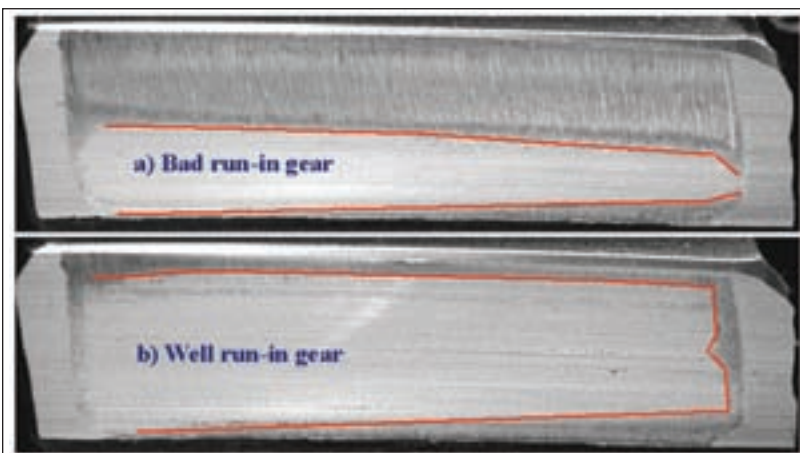


Figure 9—Scuffing.

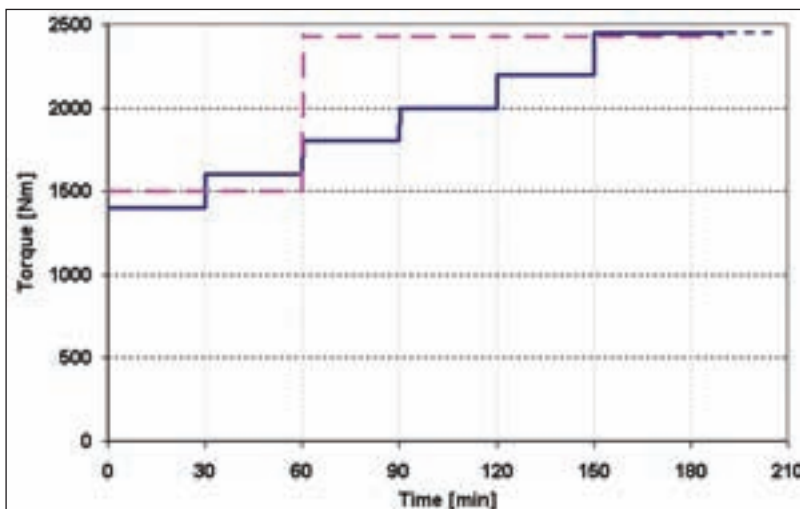


Figure 10—Two types of gear run-in.

speed (N1, N2), temperature and oil pressure (P1, P2) can be considered as global values.

The torque scanning between motor and additional gearbox (M1) is used for determining the whole circuit efficiency. This value corresponds to losses in gear assembly, bearings, coupling, etc.

Fourteen thermocouples are incorporated with the test stand, with four of them used for measurement of oil temperature in the input and output (To1, To2, T6 and T8). These values are needed for the calculation of oil heat transfer; the remaining thermocouples are magnetically fixed near the bearings.

Measured data transferred by transducers are processed by PLC, shown on a control panel screen and saved into flash memory. The PLC system also assesses adjusted value limits and, in case of its overrun, stops test processing. A good deal of important information on tested gears is provided by the measured data (Fig. 7).

**Vibration diagnostic.** It has been presumed that the application of spectral vibration analysis provides a primary indicator of pitting progress. Generated vibrations in the test gear mesh are transferred through the shaft and bearings to the gearbox, and they are measured on outer surfaces; the analyzer can be started by PLC.

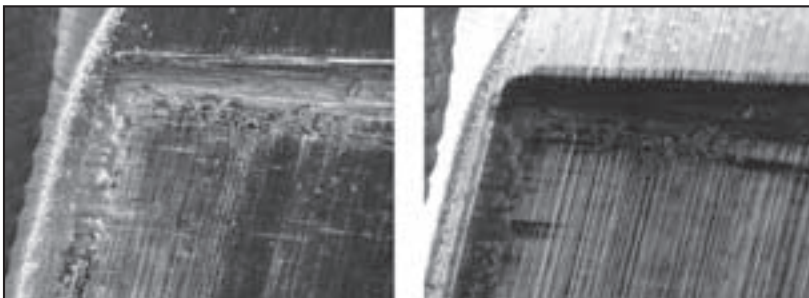


Figure 11—Comparison of two different lighting angles in picture of edge scuffing.

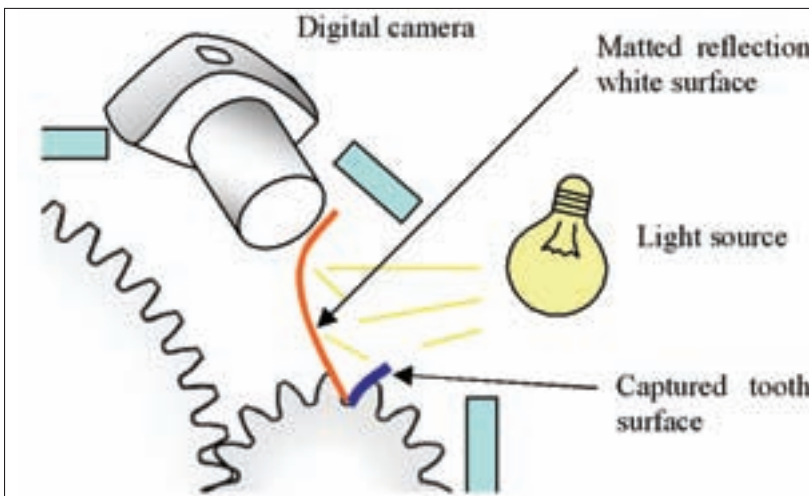


Figure 12—Suitable organization in pitting capture.

A great deal has been written (Refs. 1–2) concerning these issues. For that reason, only the diagram (Fig. 8) that originates from investigating of test rig behavior is presented.

### Scuffing Problem

Scuffing occurred at the outset of testing (Fig. 9). As scuffing influences the pitting lifetime, its elimination was necessary.

Scuffing arises when certain conditions are influenced by size of tooth line load, tooth geometry, sliding, lubrication, temperature and other factors. Test requirements did not allow changes in oil, temperature, geometry or load, etc.; eventually, a way to eliminate scuffing was determined.

With each scuffing occurrence, duration and technique of gear run-in was registered. In Figure 10, the process of run-in loading is shown. The dashed line represents the gear run-in that was used for initial research tests. In those tests, the gear run-in took one hour at normal working load and then was immediately increased to full testing load. These tests experienced scuffing. The example of tooth with scuffing failure is in Figure 9a.

The second (solid) line in Figure 10 represents a longer, more gradual run-in. The load starts on the same level and then rises by 200 Nm every half-hour, up to load testing. This probably accounts for the peaks effacement and better meshing condition, as demonstrated in Figure 9b.

### Flank Failure Evaluation

To determine the size and progress of flank damage, it is necessary to measure the damaged area objectively. In the past, the failure area was evaluated by use of a magnifying glass or macro-photography, which took too long. For that reason it has become necessary to find newer, faster and more modern methods. Vibration analysis methods may not be optimal for every application, and interpretation of results may not be exact.

Therefore the authors have developed a digital photographic method to monitor pitting expansion and pitting size, micro-pitting and scuffing failure. Its main advantages are low cost and quick turnaround.

By choosing a suitable optical system, it is possible to make an enlargement 1:200 at little cost. A disadvantage of high magnification can be a small depth and a small stop aperture setting. In order to provide maximum predictive ability, it is necessary to choose an optimal lighting angle. Two photographs of the same

pinion tooth at different lighting angles are shown in Figure 11. On this gear we studied the effect of temperature on scuffing.

### Photo Method for Pitting Evaluation

The method is based on the digital processing of captured tooth images.

Method technique:

- Capture of every tooth on analyzed gear
- Image files saved to directories with sample label and test time
- Program start
- Graphical evaluation

**Pitting record.** Pitting expansion can only be monitored if the exact distance, orientation, exposure and lighting conditions are maintained. Access openings on gearboxes must allow observation of the gear condition, picture taking and lighting; automatic evaluation is possible only with well-exposed pictures.

Generally, the capturing of a rounded metal surface, and particularly of a helical gear tooth surface, is very difficult; frequent burnouts or non-uniform lighting occur. A possible configuration is demonstrated in Figure 12.

The evaluation software developed by the authors assesses pixels with high contrast as damaged. It creates a summation of damaged and undamaged pixels and writes to a database. When an entire gear is captured and processed by the program, the database is ready to determine pitting evaluation.

**Program for image processing.** Except for image load, all program steps are automated, ensuring quality results. Even though the images are processed automatically, they can be graphically supervised by the operator (Fig. 13).

### Image processing technique:

1. Image load.
2. Compensation of image deformation caused by lens optic. (Reference grading is needed.)
3. Horizontal and vertical tooth alignment.
4. Crop the tooth surrounding.
5. Image conversion to grayscale and automatic contrast and brightness change of tone curves. This step is adjusted for best pitting dimple recognition.
6. Detection of pitting dimple edges. The Sobel method (Ref. 6) is used. It returns edges at those points where the gradient of image is a maximum. Ignored are all edges

that are not stronger than a value which is extracted from previous step. Calculation returns a binary image, with 1s where the function finds edges in image and 0s elsewhere.

7. Operations for dimple edge uniting. Controlled dilating, hole filling, image eroding, image border cleaning and removing of small objects are carried out.
8. Pits exterior boundaries trace.
9. Boundaries drawing into cropped original image (Fig. 13).
10. Pitting areas counting and area center positioning.
11. Save results in database.

**Outputs.** The main supervised output values are the total pitting damage area on one tooth  $A_{ij}$  counted in Equation (1a) and on the whole gear  $A_j$  (1b) where index  $j$  is the number of teeth and  $i$  is the number of pitting dimples. Those are required for lifetime determination. In the DIN 3990 standard, the determined value for one

continued

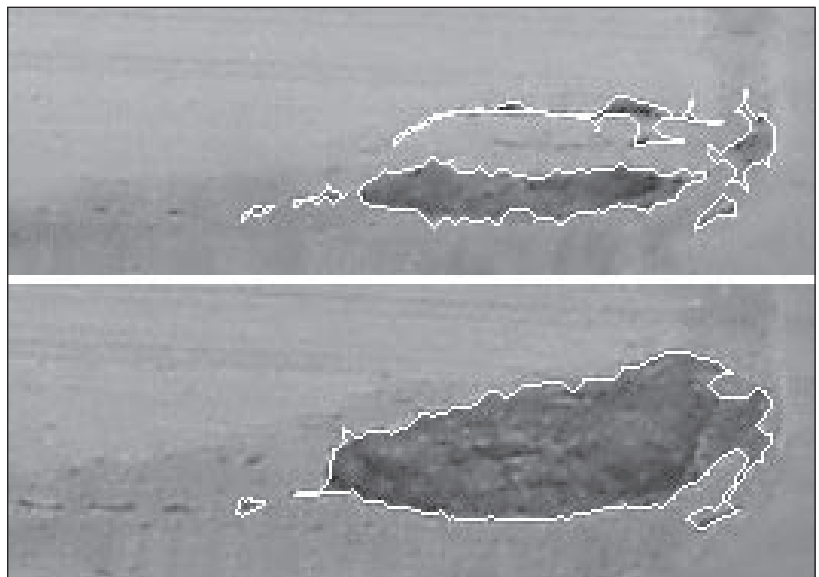


Figure 13—Example of program graphical results of two pitting stages on the same tooth.

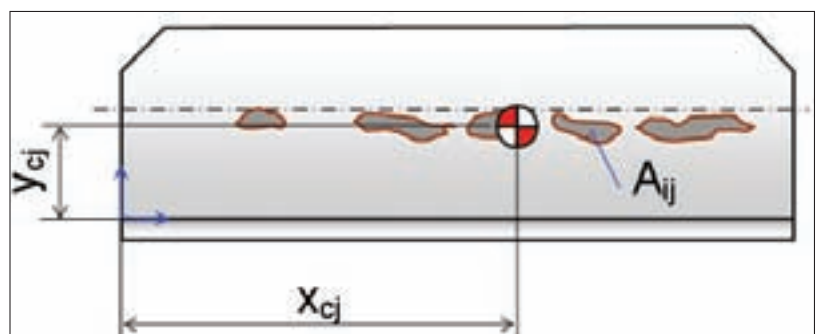


Figure 14—Center of total pitting area.

tooth is 4% surface failure of the tooth area on one tooth and 1% on the whole gear.

$$A_j = \sum A_{ij}, A = \sum A_j \quad (1)$$

The next useful value is the center of the pitting area, which serves for assessment of transverse modification suitability. Values are obtained with Equation 2 that are described in Figure 14. Those values can be converted to a percentage figure.

$$x_{ci} = \frac{\sum A_{ij} \cdot x_{ij}}{A_j}, y_{ci} = \frac{\sum A_{ij} \cdot y_{ij}}{A_j} \quad (2)$$

The relation between the total number of pitting dimples and their size can be expressed with a histogram.

**Advantages and use.** The method results are nearly exact thanks to direct measurement of the failure surface. By compliance with the aforesaid exposure demands, 6 megapixel camera and 50 mm tooth width, the resulting uncertainty is about 0.05 mm<sup>2</sup>.

Counter to perceptions, gear photo documentation is not time-consuming. For example, photo preparation and taking pictures of a gear with 16 teeth takes five minutes. Image processing is done in two minutes if a modern computer and 6 megapixel pictures are used. Compare this to the film photography and magnifying glass methods (Ref. 7), which usually take more than half-an-hour and with less precision.

It is possible to obtain a number of time-divided results in whole lifetime; the results can be statistically evaluated and the trend of pitting dimple growth can be observed in every tooth. This method is very cost-effective in comparison to vibration analysis or oil debris mass (Ref. 8) methods. It is used for specific gear lifetime determination on fatigue surface failure. Comparison of vibration or oil debris gear damage detection methods applied to pitting damage with this method is offered. The photo pitting evaluation can be applied to spur and helical gears.

### Conclusions

A gear design methodology was developed for use in the production of high-end industrial gearboxes. This method takes advantage of well-known manufactured dimensions, FEM analysis and non-standard gear profiles (especially tooth modifications).

An experimental test rig was used for

testing the shortened lifetime of gears with various geometry, material and heat processing. Vibration and a newly developed photographic method were used for pitting evaluation. The developed photographic method is helpful in the evaluation of surface failures on helical and spur gears. 

### Acknowledgments

*This work was supported by IGS CTU0711212 and MPO FT-TA2/017 grants.*

### References

1. Dempsey, P. and J. Zakrajsek. "Minimizing Load Effects on NA4 Gear Vibration Diagnostic Parameter," 2001, NASA TM—001-210671.
2. Zakrajsek, J. and D.P. Townsend. "Transmission Diagnostic Research at NASA Lewis Research Center," 1995, NASA TM—106901 ARL—TR—748.
3. Glodez, S., S. Pehan and J. Flasker. "Experimental Results of the Fatigue Crack Growth in a Gear Tooth Root," *International Journal of Fatigue*, 1998, Volume 20, Issue 9, pp. 669-675.
4. Handschuh, R. F., "Experimental Comparison of Face-Milled and Face-Hobbed Spiral Bevel Gears," NASA/TM—2001-210940 ARL—TR—1104.
5. Zak, P. and P. Jirman. "Design of Back-to-Back Testing Rig for Gear Testing," (In Czech), 2005, CTU in Prague, 01/2005/FTTA2/017.
6. Sonka, M., V. Hlavac and R. Boyle. *Image Processing, Analysis and Machine Vision*, 1998, 2nd Edition, Thomson Learning, New York.
7. Nemcekova, M. and S. Ziaran. "Alternative Diagnostic Methods for Gears Pitting," 2005, Bratislava, ISBN 80-227-2245-6, pp. 55-60.
8. Dempsey, P. J. "A Comparison of Vibration and Oil Debris Gear Damage Detection Methods Applied to Pitting Damage," 2000, NASA TM—2000-210371.

*This article first appeared in the Proceedings of IMECE 2007, the 2007 ASME International Mechanical Engineering Congress and Exposition, Nov. 11-15, 2007, Seattle, WA.*

**Pavel Žák** is a Ph.D. student working in the mechanical engineering department of the Czech Technical University in Prague. His research interests include the design and experimental evaluation of gears and transmission components. He received his Master of Science degree in engineering in 2004, also from CTU Prague.

**Dr. Vojtěch Dinybyl**, a member of the faculty of mechanical engineering at CTU Prague, is head of the university's Division of Machine Parts and Mechanisms. His research interests include design and experimental evaluation of drives, gearboxes, shafts, bearings, gears, couplings and chains. His publication credits include numerous papers on gears, gear drives and transmissions.